ORIGINAL PAPER

Myocardial work across different etiologies of right ventricular dysfunction and healthy controls

Kristoffer Berg-Hansen[1,2] · Nigopan Gopalasingam[1,2] · Tor Skibsted Clemmensen[1] · Mads Jønsson Andersen[1] · Søren Mellemkjaer[1] · Steen Hvitfeldt Poulsen[1] · Jesper Khedri Jensen[1] · Roni Nielsen[1]

Abstract

Evaluating right ventricular (RV) function remains a challenge. Recently, novel echocardiographic assessment of RV myocardial work (RVMW) by non-invasive pressure-strain loops was proposed. This enables evaluation of right ventriculoarterial coupling and quantifies RV dyssynchrony and post-systolic shortening. We aimed to assess RVMW in patients with different etiologies of RV dysfunction and healthy controls. We investigated healthy controls (n=17), patients with severe functional tricuspid regurgitation (FTR; n=22), and patients with precapillary pulmonary hypertension (PCPH; n=20). Echocardiography and right heart catheterization were performed to assess 1) RV global constructive work (RVGCW; work needed for systolic myocardial shortening and isovolumic relaxation), 2) RV global wasted work (RVGWW; myocardial shortening following pulmonic valve closure), and 3) RV global work efficiency (RVGWE; describes the relation between RV constructive and wasted work). RVGCW correlated with invasive RV stroke work index (r=0.66, $P<0.001$) and increased in tandem with higher afterload, i.e., was low in healthy controls (454±73 mmHg%), moderate in patients with FTR (687±203 mmHg%), and highest among patients with PCPH (881±255 mmHg%). RVGWE was lower and RVGWW was higher in patients with FTR (86±8% and 91 mmHg% [53-140]) or PCPH (86±10% and 110 mmHg% [66-159]) as compared with healthy controls (96±3% and 10 mmHg%). RVMW by echocardiography provides a promising index of RV function to discriminate between patients with RV volume or pressure overload. The prognostic value of this measure needs to be settled in future studies.
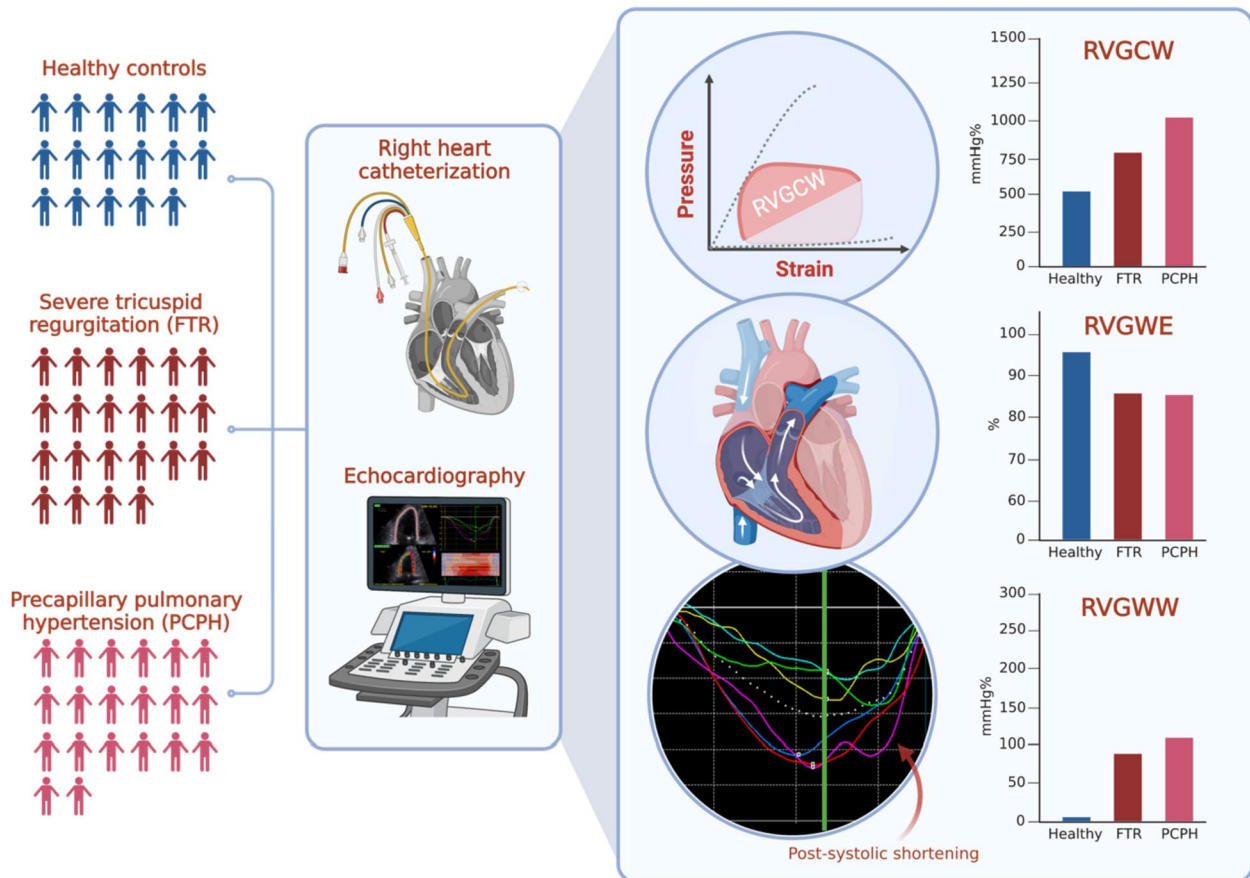
Kristoffer Berg-Hansen and Nigopan Gopalasingam have contributed equally to this work.

✉ Kristoffer Berg-Hansen
   krisbe@rm.dk

1   Department of Cardiology, Aarhus University Hospital, Palle Juul-Jensens Boulevard 99, Aarhus N DK-8200, Denmark

2   Department of Clinical Medicine, Faculty of Health, Aarhus University, Aarhus, Denmark

Graphical abstract

Combining right heart catheterization and echocardiography, right ventricular (RV) pressure-strain loops were evaluated in healthy controls and in patients with severe functional tricuspid regurgitation (FTR) or precapillary pulmonary hypertension (PCPH). RV global constructive work (RVGCW) entails the work needed for systolic myocardial shortening and isovolumic relaxation; it increased in tandem with higher afterload. RV global wasted work (RVGWW) describes myocardial shortening following pulmonic valve closure and RV global work efficiency (RVGWE) is the ratio between RVGCW and RVGWW. RVGWW was higher and RVGWE was lower in both patient groups with RV hemodynamic overload.

Introduction

Right ventricular (RV) dysfunction is a strong predictor of increased morbidity and mortality in patients with chronic elevated RV pressure or volume overload [1]. However, different etiologies of RV dysfunction may vary significantly in terms of preload, afterload, and geometric remodeling. The transition from a compensated RV to a dysfunctional RV ultimately depends on the capacity of the RV to adapt to the increased RV pressure or volume overload [2]. However, timely identification of RV dysfunction remains challenging. Echocardiographic evaluation of RV function is fundamental in evaluating right heart disease. However, traditional echocardiographic indices of RV performance are subjective to errors of angle, translational motion, and

geometric assumptions [3]. Also, echocardiographic parameters fail to assess the ventriculoarterial coupling between the RV and the pulmonary circulation; indeed, RV stroke volume is highly susceptible to changes in afterload [4]. RV global longitudinal strain (GLS) is increasingly recognized as a superior and angle-independent index of RV contractile function [5]. However, RV GLS is also load dependent and prone to error by failing to quantify contractile dyssynchrony and post-systolic shortening [6, 7]. Combining blood pressure and strain to create pressure-strain loops has been introduced as a measure of left ventricular (LV) myocardial work (LVMW) [8]. This method has been applied as a measure of RV function (RV myocardial work; RVMW) in patients with LV systolic dysfunction [9] and patients with precapillary pulmonary hypertension (PCPH) [10]. Yet, there is a paucity

of data comparing RVMW between different etiologies of RV dysfunction. In the present study, we aimed to assess pressure-strain loops in patients with PCPH or severe functional tricuspid regurgitation (FTR) and to compare RVMW between these patients and with healthy controls.

Methods

The present proof-of-concept study is an observational post-hoc investigation of two clinical trials conducted at Aarhus University Hospital between November 2017 and March 2021. Briefly, the aims of study I and II were (I) to examine the hemodynamic characteristics during rest and exercise of patients with FTR [11], and (II) to investigate the hemodynamic effects of ketone body supplements to patients with PCPH [12]. The studies were approved by the local ethics committee and the Danish Data Protection Agency. Participants were included following informed, written consent in accordance with the Helsinki Declaration. The data underlying this article will be shared upon reasonable request to the corresponding author.

Fifty-nine participants were investigated: 17 healthy controls with no cardiopulmonary disease, 22 patients with FTR secondary to clinically stable chronic atrial fibrillation, and 20 patients with PCPH (idiopathic pulmonary arterial hypertension (PAH) or chronic thromboembolic pulmonary hypertension; 10 patients in each group). For patients with PCPH, inclusion criteria were mean pulmonary arterial pressure (mPAP) > 25 mmHg, PVR > 3 Wood units, and pulmonary artery wedge pressure (PAWP) < 15 mmHg on right heart catheterization (RHC) according to the 2015 ESC guidelines on pulmonary hypertension [13]. Common exclusion criteria were LV ejection fraction (LVEF) < 50% and significant left-sided valve disease. Patients with FTR met the criteria for severe tricuspid regurgitation as outlined in the guidelines [14]; these patients were eligible for tricuspid valve repair following study participation.

A 7.5 Fr triple lumen Swan Ganz catheter was advanced through an 8 Fr sheath in the right jugular vein and advanced into the pulmonary artery by fluoroscopy guidance. All pressure recordings were evaluated in the supine position at end-expiration following a minimum of 10 min of rest. Right atrial pressure (RAP), mPAP, and PAWP were measured. Mixed venous saturation (SVO_2) was recorded. Oxygen consumption (VO_2) was measured by expired gas analysis (Vyntus CPX, Vyaire medical GMBH, Germany). The difference in arterial-venous O_2 content (A-VO_2diff) was calculated as the difference between systemic arterial and SVO_2 content. Cardiac output (CO) was calculated by direct Fick's method (CO = VO_2/A-VO_2diff) for patients with FTR and by thermodilution averaged over three consecutive measurements for healthy controls and patients with PCPH. CO was indexed relative to body surface area (BSA) as cardiac index (CI). Mean arterial blood pressure (MAP) and heart rate (HR) were measured non-invasively. Stroke volume index (SVI = CI/HR), PVR ([mPAP-PAWP]/CO), pulmonary arterial compliance (PAC = SV/pulmonary arterial pulse pressure), and RV stroke work index (RVSWI = SVI × [mPAP-RAP] × 0.0136) were calculated [15, 16].

2D echocardiograms were attained with a 3.5 MHz transducer on a GE vivid E95 (GE Healthcare, USA). Echocardiography was performed immediately following the invasive measurements. All images were stored digitally and analyzed post-hoc with EchoPAC software (General Electric Vingmed Ultrasound, USA). The echocardiographic measures were averaged over 3 consecutive beats at sinus rhythm or 4–6 beats at atrial fibrillation. RV parameters were calculated according to guidelines from an RV-focused apical view [17]. RV GLS, free wall strain (FWS), tricuspid annular peak systolic velocity (RV S'), tricuspid annular plane systolic excursion (TAPSE), and RV fractional area change (RV FAC) were measured [17]. GLS measures are reported as absolute values. Pulmonary arterial systolic pressure (PASP) was assessed by applying the Bernoulli equation to the tricuspid regurgitant jet peak velocity, and RAP was added. The TAPSE/PASP-ratio was calculated [18]. LVEF was calculated by Simpson biplane method and GLS was calculated from LV-focused apical views using a 17-segment model.

The novel indices of RV myocardial work were analyzed using specialized software designed to acquire LV myocardial work by combining two-dimensional speckle tracking echocardiography and blood pressure (EchoPAC Version 204). This enabled the synchronization of RV GLS values with simultaneous invasively measured pulmonary pressures. First, RV GLS was attained, followed by cardiac cycle timing with the pulmonic (through a pulsed-wave doppler in the RV outflow tract) and tricuspid valves (through visual rectification) combined with pulmonary pressures; RV pressure-strain loops were constructed within the software (Fig. 1). Four parameters were attained: (1) RV global work index (RVGWI; mmHg%), (2) RV global constructive work (RVGCW; mmHg%), (3) RV global wasted work (RVGWW; mmHg%), and (4) RV global work efficiency (RVGWE; %). RVGWI describes the area calculated from tricuspid valve closure to opening within the global RV pressure-strain loop; RVGCW describes the work needed for systolic myocardial shortening and isovolumic relaxation; RVGWW describes the wasted work during each cardiac cycle (i.e., myocyte lengthening during systole and shortening during isovolumic relaxation); and RVGWE describes the relation between RVGCW and the sum of RVGCW and RVGWW.

Continuous data are presented as mean and standard deviation or median and interquartile range, while categorical variables are presented as number and frequency. Normality
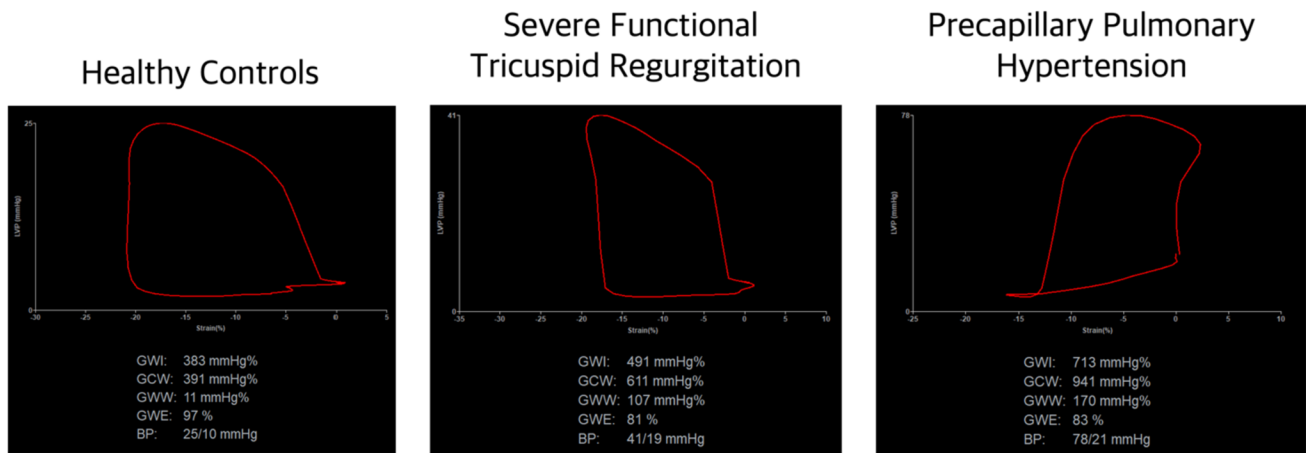
Fig. 1 Representative pressure-strain loops from healthy controls and patients with severe functional tricuspid regurgitation or precapillary pulmonary hypertension

distribution was assessed by QQ-plots and histograms. For comparisons among groups, continuous data were compared using the one-way ANOVA test for normal distributed data, and the Kruskal-Wallis test for non-parametric data. The chi-squared test was performed for categorical data. Pearson's coefficient was used to assess correlation between continuous variables. Inter- and intraobserver agreement of RVMW in patients with PCPH (n = 9) or FTR (n = 10) were assessed by Bland-Altman plots and intraclass correlation coefficients (ICC). Thus, patient exams were selected in random to assess the reproducibility of RVMW. A two-sided P-value < 0.05 was considered statistically significant. Statistical tests were performed using STATA version 16 (StataCorp LP, Texas). Figures were created in GraphPad Prism 9.2 (GraphPad Software, California).

Results

Patient characteristics are presented in Table 1. Age differed between the groups; healthy controls were younger ($P < 0.001$) and patients with FTR were older than patients with PCPH ($P < 0.001$). Comorbidities were equally distributed between patients with FTR and PCPH, except for an increased prevalence of hypertension in patients with FTR ($P = 0.01$). Patients with FTR received more frequently antihypertensive and anticoagulant medication, in addition with diuretics. Meanwhile, patients with PCPH received guideline recommended medication as appropriate (Supplementary Table 1). Finally, N-terminal pro brain-natriuretic-peptide (NT-proBNP) was significantly higher among patients with FTR as compared with PCPH patients ($P < 0.001$). Five patients with FTR (23%) and 2 patients with PCPH (10%) had RBBB.

The echocardiographic parameters are presented in Table 2. RV GLS was reduced in both patient categories as compared with healthy controls ($P < 0.001$), however, there was no significant difference between patients with FTR and PCPH. Meanwhile, RV FWS, TAPSE, and TAPSE/PASP-ratio differed between all three study groups: these were highest in healthy controls, lower in patients with FTR, and lowest among patients with PCPH ($P < 0.001$ for all parameters). LVEF was significantly lower in patients with FTR compared with controls, while no significant difference in LV GLS was observed. LV hypertrophy was more pronounced in patients with FTR compared with the other study groups ($P < 0.001$).

RVMW parameters derived from pressure-strain calculations are displayed in Table 2; Fig. 2. RVGWI ($P = 0.02$) and RVGCW ($P = 0.003$) were significantly higher in patients with PCPH compared with FTR patients. RVGCW and RVGWW were greater in both patient groups as compared with controls ($P < 0.001$ for both values). In parallel, RVGWE was reduced in both patient groups compared with controls ($P < 0.001$). After adjusting for age, sex, and body mass index (BMI) RVGWE remained significantly reduced in patients with PCPH ($7.9 \pm 3.2\%$, $P = 0.02$), but not in patients with FTR ($3.5 \pm 3.9\%$, $P = 0.37$) as compared with controls. RVGWE was independently influenced by age; for every 1-year increment in age RVGWE decreased by 0.19 ± 0.8 ($P = 0.02$) percentage points (Supplementary Table 2).

There was no significant difference in CI, SVI, and SVO_2 between patients with FTR or PCPH, whereas mPAP, PVR, and RVSWI were higher in the latter study group ($P < 0.001$ for all parameters; Table 3). RAP and PAWP were elevated in patients with FTR compared with patients with PCPH ($P < 0.001$).

Table 1 Baseline characteristics

	Healthy controls (n=17)	FTR (n=22)	PCPH (n=20)	P-value
Age, years	49 ± 13	78 ± 5[†]	59 ± 17[−†‡]	< 0.001
Male Sex	12 (71%)	11 (50%)	5 (25%)[†‡]	0.021
BMI, kg/m²	24 ± 2	28 ± 5[†]	26 ± 5	0.013
NYHA/WHO-class I/II/III, n	–	1/10/11	3/14/3	0.046
Comorbidities				
Hypertension	–	13 (59%)	4 (20%)	0.010
Dyslipidemia	–	7 (32%)	3 (15%)	0.201
Diabetes Mellitus	–	4 (18%)	0	0.063
Ischemic Heart Disease	–	2 (9%)	0 (0%)	0.167
CKD (eGFR < 60 mL/min/1.73 m²)	–	8 (36%)	6 (30%)	0.662
Medication				
ACEi or ARB	–	10 (45%)	3 (15%)	0.033
Betablockers	–	12 (55%)	0 (0%)	< 0.001
Loop Diuretics	–	17 (77%)	9 (45%)	0.031
Mineralocorticoid receptor antagonist	–	7 (32%)	1 (5%)	0.027
Oral Anticoagulation	–	21 (95%)	13 (65%)	0.012
Calcium channel blockers	–	8 (38%)	1 (6%)	0.020
Laboratory data				
NT-proBNP, pmol/L	37 (34, 96)	1245 (817, 1849)[†]	466 (132, 635)[†‡]	< 0.001
eGFR, mL/min/1.73 m²	92 ± 11	68 ± 20[†]	79 ± 28	0.006
Hemoglobin, mmol/L	9.0 ± 0.9	8.4 ± 0.9	9.0 ± 0.9	0.063

Values are n (%), mean ± SD or median (interquartile range)

ACEi angiotensin-converting enzyme inhibitor, *ARB* angiotensin receptor blocker, *CKD* chronic kidney disease, *eGFR* estimated glomerular filtration rate, *FTR* functional tricuspid regurgitation, *NT-proBNP* N-terminal pro brain-natriuretic-peptide, *NYHA* New York Heart Association, *PCPH* precapillary pulmonary hypertension, *WHO* World Health Organization

[†]Significantly different versus controls

[†‡]Significantly different versus FTR

The novel method of RV pressure-strain loops was compared to an invasively measured index of right ventriculoarterial coupling, namely RVSWI. In a pooled analysis, there was a good correlation between RVGCW and RVSWI (r = 0.66, *P* < 0.001; Fig. 3), however this was only confirmed in patients with PCPH (r = 0.62, *P* = 0.004; Table 4). Meanwhile, there was no significant correlation between RVGCW and RVSWI in controls (r = 0.36, *P* = 0.20) or patients with FTR (r = 0.11, *P* = 0.62; Table 4). RVGCW was highly dependent on RV afterload and correlated significantly with mPAP (r = 0.80, *P* < 0.001), PVR (0.74, *P* < 0.001), and PAC (−0.63, *P* < 0.001; Supplementary Fig. 1). In patients with PCPH, RV FWS showed mild correlation with RVSWI, while no correlation was apparent in the other study groups (Table 4). Other echocardiographic parameters did not correlate significantly with RVSWI (Table 4).

RVGCW (r = 0.47, *P* = 0.04) and RVGWI (r = 0.66, *P* = 0.002) correlated with SVI in patients with PCPH (Supplementary Fig. 2), with no apparent correlation in the other study groups. However, this was not directly related

to increased afterload, as there was no significant correlation between SVI and indices of RV afterload, i.e., mPAP (r = 0.27, *P* = 0.26) and PVR (0.15, *P* = 0.52) in patients with PCPH. We found no correlation between PVR and RVGWE nor RVGWW.

Bland-Altman plots for the assessment of inter- and intraobserver variability in patients with FTR and PCPH are shown in Supplementary Fig. 3. In patients with FTR, ICC for interobserver variability was 0.84 (95%CI 0.30–0.96) for RVGWI (*P* = 0.008), 0.88 (95%CI 0.54–0.97) for RVGCW (*P* = 0.002), 0.83 (95%CI 0.35–0.96) for RVGWW (*P* = 0.005), and 0.92 (95%CI 0.71–0.98) for RVGWE (*P* < 0.001); ICC for intraobserver variability was 0.87 (95%CI 0.50–0.97) for RVGWI (*P* = 0.002), 0.95 (95%CI 0.80–0.99) for RVGCW (*P* < 0.001), 0.95 (95%CI 0.80–0.99) for RVGWW (*P* < 0.001), and 0.88 (95%CI 0.56–0.88) for RVGWE (*P* = 0.001; Supplementary Table 3). In patients with PCPH, ICC for interobserver variability was 0.87 (95%CI 0.39–0.97) for RVGWI (*P* = 0.006),

Table 2 Echocardiographic parameters

|	Healthy controls (n=17)	FTR (n=22)	PCPH (n=20)	P-value
RVGWI, mmHg%	417±73	508±179	646±242[†‡]	0.003
RVGCW, mmHg%	454±73	687±203[†]	881±255[†‡]	<0.001
RVGWW, mmHg%	10 (6, 17)	91 (53, 140)[†]	110 (66, 159)[†]	<0.001
RVGWE, %	96±3	86±8[†]	86±10[†]	<0.001
TAPSE/PASP, mm/mmHg*	1.34±0.39	0.78±0.35[†]	0.43±0.32[†‡]	<0.001
RV GLS, %	23.7±3.2	16.7±4.0[†]	15.9±3.4[†]	<0.001
RV FWS, %	27.8±3.9	21.8±4.8[†]	16.5±4.6[†‡]	<0.001
RV S', cm/sec	11.6±1.6	11.2±1.7	11.7±3.5	0.78
TAPSE, mm	27±3	21±4[†]	16±4[†‡]	<0.001
RV FAC, %	46.2±6.2	37.9±6.4[†]	29.5±11.4[†‡]	<0.001
RV Basal Diameter, mm	35±2	51±7[†]	47±6[†]	<0.001
RV Mid Diameter, mm	27±3	42±10[†]	38±7[†]	<0.001
LVEF, %	63±5	59±5[†]	58±7[†]	0.021
LV GLS, %	20±2	17±3	18±3	0.051
LV Mass Index, g/m²	77±14	96±24†	71±22[‡]	<0.001

Values are mean±SD or median (interquartile range)

LVEF left ventricular (LV) ejection fraction, *LV GLS* LV global longitudinal strain, *PASP* pulmonary artery systolic pressure, *RV FAC* RV fractional area change, *RV FWS* RV free wall longitudinal strain, *RV GLS* RV global longitudinal strain, *RVGCW and RVGWW* RV global constructive and wasted work, *RVGWE and RVGWI* RV global work efficiency and index, *RV S'* tricuspid annular peak systolic velocity, *TAPSE* tricuspid annular plane systolic excursion. Other abbreviations as in Table 1

*Available in 44/59 (75%) echocardiographic exams

[†]Significantly different versus controls

[†‡]Significantly different versus FTR
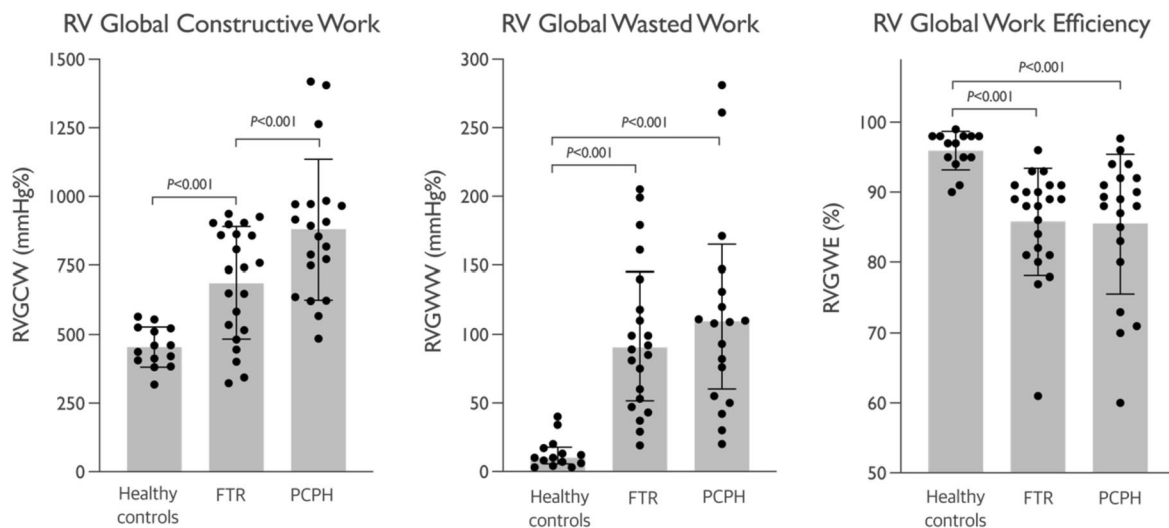
Fig. 2 RV global constrictive, wasted, and work efficiency in patients with FTR or PCPH and healthy controls

0.81 (95%CI 0.23–0.96) for RVGCW ($P = 0.01$), 0.71 (95%CI −0.21–0.93) for RVGWW ($P = 0.04$), and 0.81 (95%CI 0.20–0.96) for RVGWE ($P = 0.01$); ICC for intraobserver variability was 0.90 (95%CI 0.59–0.98) for RVGWI ($P = 0.001$), 0.92 (95%CI 0.61–0.98) for RVGCW ($P = 0.002$), 0.50 (95%CI −0.58–0.88) for RVGWW ($P = 0.13$), and 0.88 (95%CI 0.49–0.97) for RVGWE ($P = 0.003$; Supplementary Table 3).

Table 3 Right heart catheterization parameters

	Healthy controls (n=17)	FTR (n=22)	PCPH (n=20)	*P*-value
Heart Rate, min^{-1}	63 ± 9	74 ± 14[†]	70 ± 10	0.033
MAP, mmHg	92 ± 10	101 ± 16	93 ± 12	0.080
CI, L/min/m^2	3.1 ± 0.6	2.2 ± 0.5[†]	2.3 ± 0.4[†]	< 0.001
SVI, mL/m^2	48.8 ± 9.5	25.9 ± 7.6[†]	34.1 ± 6.7[†‡]	< 0.001
RVSWI, g m/m^2/beat	6.8 ± 1.5	5.7 ± 2.9	16.4 ± 6.1[†‡]	< 0.001
RAP, mmHg	5 ± 2	12 ± 5[†]	5 ± 4[‡]	< 0.001
mPAP, mmHg	15 ± 2	28 ± 8[†]	39 ± 10[†‡]	< 0.001
PCWP, mmHg	9 ± 2	17 ± 5[†]	10 ± 4[‡]	< 0.001
PVR, WU	1.2 ± 0.3	2.7 ± 1.2[†]	7.1 ± 2.4[†‡]	< 0.001
PAC, mL/mmHg	8.5 ± 2.4	2.2 ± 1.1[†]	1.8 ± 0.8[†]	< 0.001
SVO$_2$, %	76 ± 4	65 ± 5[†]	66 ± 5[†]	< 0.001

Values are mean ± SD or median (interquartile range)

CI cardiac index, *MAP* mean arterial pressure, *mPAP* mean pulmonary arterial pressure, *PAC* pulmonary artery compliance, *PCWP* pulmonary capillary wedge pressure, *PVR* pulmonary vascular resistance, *RAP* right atrial pressure, *RVSWI* right ventricular stroke work index, *SVI* stroke volume index, *SVO$_2$* mixed venous oxygen saturation. Other abbreviations as in Table 1

[†]Significantly different versus controls

[†‡]Significantly different versus FTR
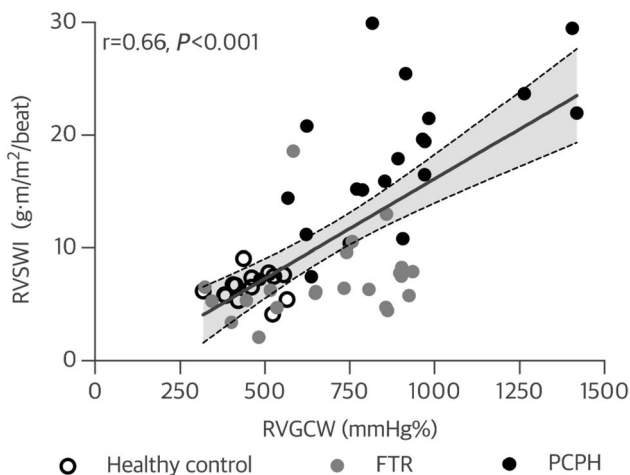

Fig. 3 Correlation between RV global constructive work and RV stroke work index

Discussion

In this study, we investigated RV function by integrating strain and pulmonary pressure to assess RVMW by pressure-strain loops in patients with RV hemodynamic overload and healthy controls. The main findings were: (1) RVGCW increased in tandem with higher afterload, i.e., was low among healthy controls, moderate in patients with FTR (i.e., RV volume overload), and highest among patients with PCPH (i.e., RV pressure overload); (2) RVGCW was highly dependent on RV afterload and correlated well with invasively measured RVSWI among patients with PCPH, but not in patients with FTR; (3) RVGWE was lower and RVGWW was higher among patients with FTR or PCPH compared to healthy control subjects, however, in patients with FTR this was partly explained by older age; (4) There was modest to good

Table 4 Correlation between echocardiographic parameters and right ventricular stroke work index within each study group

RVSWI (g m/m^2/beat)	Healthy controls (n=17)			FTR (n=22)			PCPH (n=20)		
	ρ	ß (SE)	*P* value	ρ	ß (SE)	*P* value	ρ	ß (SE)	*P* value
RVGCW, mmHg%	0.36	17.7 (13.0)	0.20	0.11	7.9 (15.9)	0.62	0.62	25.8 (7.8)	0.004
TAPSE/PASP, mm/mmHg	− 0.32	− 0.1 (0.1)	0.34	− 0.1	− 0.01 (0.01)	0.71	− 0.29	− 0.02 (0.02)	0.43
TAPSE, mm	0.41	0.9 (0.5)	0.12	0.17	0.3 (0.3)	0.45	0.33	0.2 (0.1)	0.15
RV FWS, %	− 0.29	− 17.4 (16.8)	0.32	− 0.08	− 7.0 (20.9)	0.74	− 0.55	− 24.6 (9.2)	0.02
RV GLS, %	− 0.20	− 0.4 (0.6)	0.49	0.20	0.3 (0.3)	0.43	− 0.13	− 0.1 (0.1)	0.58
RV S', cm/sec	N/A	N/A	N/A	− 0.11	− 0.1 (0.1)	0.65	0.08	0.1 (0.1)	0.76

Abbreviations as in Table 2

inter- and intraobserver repeatability of most RVMW parameters in patients with FTR and PCPH.

The RV possesses a unique ability to adapt to immense chronic increases in afterload by augmenting contractility to preserve cardiac output [19]. Therefore, both contractility and afterload (i.e., right ventriculoarterial coupling) must be assessed to evaluate RV dysfunction. RVSWI reflects the area inside the RV pressure-volume loop and comprises ventricular stroke volume in combination with preload and afterload. It is closely correlated with myocardial oxygen consumption and reflects the ventricular work to produce hydraulic energy, generating forward stroke work [20]. Several studies on patients with PCPH report decreased RVSWI to be independently associated with increased mortality [21, 22]. These findings reflect the transition from clinically compensated homeometric RV adaptation (i.e., increased contractility to match augmented afterload) to decompensated heterometric maladaptation (i.e., contractility is unable to match afterload, resulting in "ventriculoarterial uncoupling") [23]. We observed a good correlation between RVSWI and echocardiographic-derived RVGCW in patients with PCPH, but not in patients with FTR. This may be explained by the regurgitant volume from the RV to the right atrium that contributes to the overall RV stroke work in patients with FTR. Consequently, this is better captured by RVGCW rather than RVSWI alone which is closely linked to forward stroke volume. Thus, by implementing valvular event-timings, RVGCW closely reflects RV stroke work, disregarding ventricular dyssynchrony and post-systolic contraction as wasted work. Distinct values of RVGCW were demonstrated within each study group. Evaluating RVGCW may thus aid to assess RV dysfunction in different right heart pathologies. Furthermore, RVGCW may serve as an integrative index of right ventriculoarterial coupling to monitor treatment response and disease progression in patients with RV hemodynamic overload. There was an apparent correlation between RVGCW and indices of RV afterload. As the patients with PCPH were stable, this finding may reflect preserved right ventriculoarterial coupling in these patients, i.e., homeometric RV adaptation to chronic pressure overload. Indeed, RVGCW was found to correlate with stroke volume in these patients. Hence, myocardial function (as measured with longitudinal strain) was sufficient to match the increase in afterload, and so, echocardiographic pressure-strain measurements associated with invasively measured pressure-flow measurements (i.e., RVSWI). Meanwhile, patients with FTR had higher RV filling pressures and increased indices of RV end-diastolic volume, in addition to increased FAC, all of which may indicate heterometric maladaptation [2]. Stroke volume and RVSWI were reduced, while RVGCW remained increased (relative to

healthy controls), indicating increased RV work in the presence of increased backward flow. Therefore, monitoring RVGCW may aid in assessing progression of RV dysfunction in patients with FTR.

RV mechanical dyssynchrony comprises an important pathophysiological feature in PCPH [6]. Delayed time-to-peak contraction of the RV is evident in PAH [24, 25], causing mechanically inefficient post-systolic isovolumetric contraction (i.e., wasted contractile work) [26]. In agreement with the literature, we discovered an increase in RV wasted work in both patient categories of RV hemodynamic overload. Consequently, RVGWE was impaired, consistent with RV mechanical inefficiency due to chronic hemodynamic overload. As RVGWE is dependent on the RV constructive-to-wasted work ratio, it reflects the mechanical determinants of this relationship, especially, forward stroke work and inefficient post-systolic shortening. By accounting for and quantifying the magnitude of the prolonged post-systolic period, RVGWW may reflect the degree of RV electromechanical dyssynchrony. Indeed, the degree of RV dyssynchrony correlates with the severity of PCPH, distinguishing healthy controls from borderline and manifest PAH [6, 19, 27]. Thus, impaired RVGWE during follow-up of patients with PCPH may reflect disease progression including RV dysfunction due to either increased wasted work, reduced constructive work, or both combined. Echocardiographic assessment of RV dysfunction remains challenging due to the intrinsic right ventriculoarterial relationship and complex ventricular anatomy. TAPSE and S' are well-validated and easily obtained measures of RV systolic function. However, they are dependent on cardiac angle and motion relative to the ultrasound transducer [28]. Next, RV longitudinal strain is a reproducible measure of RV systolic function and shows prognostic value in patients with PAH or FTR [29, 30]. Yet, it is load dependent, limiting the evaluation of PAH [31]. Validation of three-dimensional echocardiographic RV ejection fraction versus CMR has shown promising results [32] but is hampered by imperfect image quality, load dependency, possible severe TR, and interventricular dyssynchrony causing septal bouncing [17, 18]. TAPSE/PASP-ratio has been utilized to evaluate right ventriculoarterial coupling in patients with severe FTR, demonstrating prognostic information [18]. Nevertheless, the TAPSE/PASP-ratio is limited by the abovementioned limitations. In this regard, we found no correlation between TAPSE/PASP-ratio and RVSWI in patients with FTR or PCPH. By incorporating both contractile function and afterload, RVMW provides a less load dependent index of ventricular performance. We discovered highly comparable values of RVGWI, RVGCW, RVGWW, and RVGWE in healthy controls and patients with PCPH as previously reported [9, 10]. Furthermore, inter- and intraobserver variability was modest to good except for RVGWW, which may be limited by imperfect valvular event timing

and small values. In the present study, we provide information that extends the generalizability of RVMW to patients with various forms of RV hemodynamic overload, including RV pressure and volume overload. Importantly, these measures can be easily incorporated into clinical practice, as they require minimal extra acquisition time and demonstrate good reproducibility, including consistent results across different laboratories [10].

Due to the cross-sectional design of this study, potential limitations should be considered. First, disease duration remains unknown and cannot be accounted for. Second, despite an association between RVGCW and RVSWI, correlation does not necessitate causation. Third, because of the retrospective nature of this investigation, study groups were heterogeneous with respect to baseline characteristics, including differences in age, sex distribution, and BMI. Nevertheless, each study group was internally homogenous with respect to baseline characteristics and hemodynamic profiles and the healthy control demonstrated no signs of RV volume overload. Moreover, our results align with those reported by Butcher et al. [10], and reinforces the external validity and reproducibility of echocardiographic indices of RV myocardial work. The present data are based on combining echocardiographic RV longitudinal strain and invasive measures of pulmonary pressures. Hence, RHC was presupposed. Whether non-invasive derived pulmonary pressures would produce similar results remain undetermined. However, this may only be feasible in selected patients in whom TR flow velocity can be measured validly without a laminar flow profile. Another limitation is that RVMW was evaluated using software originally created and tested for evaluation of LVMW [8]. Patients with FTR had chronic atrial fibrillation. As the evaluation of RVMW requires valvular event timings, variation in cardiac cycle length may pose a potential limitation. Still, we observed good interobserver agreement in the RVMW measurements in these patients. Moreover, studying FTR in patients with atrial fibrillation is highly relevant, as these patients represent the majority of patients with FTR [33]. Finally, LV pressure-strain loops are validated by invasive pressure-volume loops, using brachial artery blood pressure and simple geometric assumptions [8]. The irregular RV geometry challenges these assumptions, making volumetric assessment difficult [2]. Despite this, RV pressure-strain loops rely less on volume by measuring longitudinal force-segment changes. Future trials are crucial for exploring the correlation between invasive RV pressure-volume and pressure-strain loops using echocardiography.

In conclusion, assessment of RVMW is feasible in patients with RV hemodynamic overload and differs from healthy controls. RVGCW correlates well with invasive assessment of RVSWI in patients with RV pressure overload but not in patients with RV volume overload. Furthermore, this method enables quantification of RVGWW and RVGWE. Whether this novel method possesses prognostic value, and whether it can be applied to assess specific treatment effects and disease progression needs to be determined in long-term future studies.

Declarations

Competing interests No conflict of interest declared.

References

1. Konstam MA, Kiernan MS, Bernstein D, Bozkurt B, Jacob M, Kapur NK et al (2018) Evaluation and management of right-sided heart failure: a scientific statement from the american heart association. Circulation 137:e578
2. Sanz J, Sánchez-Quintana D, Bossone E, Bogaard HJ, Naeije R (2019) Anatomy, function, and dysfunction of the right ventricle: JACC state-of-the-art review. J Am Coll Cardiol 73:1463–1482
3. Rudski LG, Lai WW, Afilalo J, Hua L, Handschumacher MD, Chandrasekaran K et al (2010) Guidelines for the echocardiographic assessment of the right heart in adults: a report from the American society of echocardiography endorsed by the European

association of echocardiography, a registered branch of the European society of cardiology, and Canadian society of echocardiography. J Am Soc Echocardiogr 23:685–688

4. MacNee W (1994) Pathophysiology of cor pulmonale in chronic obstructive pulmonary disease. Part one. Am J Respir Crit Care Med 150:833–852

5. Houard L, Benaets MB, de Meester de Ravenstein C, Rousseau MF, Ahn SA, Amzulescu MS et al (2019) Additional prognostic value of 2D right ventricular speckle-tracking strain for prediction of survival in heart failure and reduced ejection fraction: a comparative study with cardiac magnetic resonance. JACC Cardiovasc Imaging 12:2373–2385

6. Badagliacca R, Poscia R, Pezzuto B, Papa S, Gambardella C, Francone M et al (2015) Right ventricular dyssynchrony in idiopathic pulmonary arterial hypertension: determinants and impact on pump function. J Heart Lung Transplant 34:381–389

7. Aalen J, Storsten P, Remme EW, Sirnes PA, Gjesdal O, Larsen CK et al (2019) Afterload hypersensitivity in patients with left Bundle Branch Block. JACC Cardiovasc Imaging 12:967–977

8. Russell K, Eriksen M, Aaberge L, Wilhelmsen N, Skulstad H, Remme EW et al (2012) A novel clinical method for quantification of regional left ventricular pressurestrain loop area: a non-invasive index of myocardial work. Eur Heart J 33:724–733

9. Butcher SC, Fortuni F, Montero-Cabezas JM, Abou R, El Mahdiui M, van der Bijl P et al (2020) Right ventricular myocardial work: proof-of-concept for non-invasive assessment of right ventricular function. Eur Hear J Cardiovasc Imaging 22:142

10. Butcher SC, Feloukidis C, Kamperidis V, Yedidya I, Stassen J, Fortuni F et al (2022) Right ventricular myocardial work characterization in patients with pulmonary hypertension and relation to invasive hemodynamic parameters and outcomes. Am J Cardiol 177:151–161

11. Jensen JK, Clemmensen TS, Frederiksen CA, Schofer J, Andersen MJ, Poulsen SH (2021) Clinical performance and exercise hemodynamics in patients with severe secondary tricuspid regurgitation and chronic atrial fibrillation. BMC Cardiovasc Disord England 21:276

12. Nielsen R, Christensen KH, Gopalasingam N, Berg-Hansen K, Seefeldt J, Homilius C et al (2023) Hemodynamic effects of ketone bodies in patients with pulmonary hypertension. J Am Heart Assoc England 12:e028232

13. Galiè N, Humbert M, Vachiery JL, Gibbs S, Lang I, Torbicki A et al (2016) 2015 ESC/ERS guidelines for the diagnosis and treatment of pulmonary hypertension. Eur Heart J 37:67–119

14. Vahanian A, Beyersdorf F, Praz F, Milojevic M, Baldus S, Bauersachs J et al (2022) 2021 ESC/EACTS Guidelines for the management of valvular heart disease: developed by the task force for the management of valvular heart disease of the European society of cardiology (ESC) and the European association for cardio-thoracic surgery (EACTS). Eur Heart J 43:561–632. https://doi.org/10.1093/eurheartj/ehab395

15. Mahajan A, Shabanie A, Varshney SM, Marijic J, Sopher MJ (2007) Inhaled nitric oxide in the preoperative evaluation of pulmonary hypertension in heart transplant candidates. J Cardiothorac Vasc Anesth 21:51–56

16. Thenappan T, Prins KW, Pritzker MR, Scandurra J, Volmers K, Weir EK (2016) The critical role of pulmonary arterial compliance in pulmonary hypertension. Ann Am Thorac Soc 13:276–284

17. Lang RM, Badano LP, Mor-Avi V, Afilalo J, Armstrong A, Ernande L et al (2015) Recommendations for cardiac chamber quantification by echocardiography in adults: an update from the American society of echocardiography and the European association of cardiovascular imaging. J Am Soc Echocardiogr 28:1-39e14

18. Brener MI, Lurz P, Hausleiter J, Rodés-Cabau J, Fam N, Kodali SK et al (2022) Right ventricular-pulmonary arterial coupling and afterload reserve in patients undergoing transcatheter tricuspid valve repair. J Am Coll Cardiol 79:448–461

19. Vonk Noordegraaf A, Westerhof BE, Westerhof N (2017) The Relationship between the right ventricle and its load in pulmonary hypertension. J Am Coll Cardiol 69:236–243

20. Suga H (1979) Total mechanical energy of a ventricle model and cardiac oxygen consumption. Am J Physiol 236:H498-505

21. Brittain EL, Pugh ME, Wheeler LA, Robbins IM, Loyd JE, Newman JH et al (2013) Shorter survival in familial versus idiopathic pulmonary arterial hypertension is associated with hemodynamic markers of impaired right ventricular function. Pulm Circ 3:589–598

22. Clapham KR, Highland KB, Rao Y, Fares WH (2020) Reduced RVSWI is associated with increased mortality in connective tissue disease associated pulmonary arterial hypertension. Front Cardiovasc Med 7:77

23. Lahm T, Douglas IS, Archer SL, Bogaard HJ, Chesler NC, Haddad F et al (2018) Assessment of right ventricular function in the research setting: knowledge gaps and pathways forward an official American thoracic society research statement. Am J Respir Crit Care Med 198:e15–43

24. Marcus JT, Gan CTJ, Zwanenburg JJM, Boonstra A, Allaart CP, Götte MJW et al (2008) Interventricular mechanical asynchrony in pulmonary arterial hypertension. Left-to-right delay in peak shortening is related to right ventricular overload and left ventricular underfilling. J Am Coll Cardiol 51:750–757

25. Kalogeropoulos AP, Georgiopoulou VV, Howell S, Pernetz MA, Fisher MR, Lerakis S et al (2008) Evaluation of right intraventricular dyssynchrony by two-dimensional strain echocardiography in patients with pulmonary arterial hypertension. J Am Soc Echocardiogr 21:1028–1034

26. Gan CT-J, Lankhaar J-W, Marcus JT, Westerhof N, Marques KM, Bronzwaer JGF et al (2006) Impaired left ventricular filling due to right-to-left ventricular interaction in patients with pulmonary arterial Hypertension. Am J Physiol Heart Circ Physiol 290:H1528–H1533

27. Lamia B, Muir JF, Molano LC, Viacroze C, Benichou J, Bonnet P et al (2017) Altered synchrony of right ventricular contraction in borderline pulmonary Hypertension. Int J Cardiovasc Imaging 33:1331–1339

28. Giusca S, Dambrauskaite V, Scheurwegs C, D'Hooge J, Claus P, Herbots L et al (2010) Deformation imaging describes right ventricular function better than longitudinal displacement of the tricuspid ring. Heart 96:281–288

29. Haeck MLA, Scherptong RWC, Marsan NA, Holman ER, Schalij MJ, Bax JJ et al (2012) Prognostic value of right ventricular longitudinal peak systolic strain in patients with pulmonary Hypertension. Circ Cardiovasc Imaging 5:628–636

30. Ancona F, Melillo F, Calvo F, Attalla El Halabieh N, Stella S, Capogrosso C et al (2021) Right ventricular systolic function in severe tricuspid regurgitation: prognostic relevance of longitudinal strain. Eur Heart J Cardiovasc Imaging 22:868–875

31. Wright L, Negishi K, Dwyer N, Wahi S, Marwick TH (2017) Afterload dependence of right ventricular myocardial strain. J Am Soc Echocardiogr Off Publ Am Soc Echocardiogr 30:676-684e1

32. Sugeng L, Mor-Avi V, Weinert L, Niel J, Ebner C, Steringer-Mascherbauer R et al (2010) Multimodality Comparison of Quantitative Volumetric Analysis of the right ventricle. JACC Cardiovasc Imaging 3:10–18

33. Fender EA, Zack CJ, Nishimura RA (2018) Isolated tricuspid regurgitation: outcomes and therapeutic interventions. Heart 104:798–806